International Conference on Space Optics—ICSO 2018

Chania, Greece

9–12 October 2018

Edited by Zoran Sodnik, Nikos Karafolas, and Bruno Cugny

Detection efficiency of micro channel plates and channel electron multiplier detectors to penetrating radiation in Space

N. André

A. Fedorov

O. Chassela

A. Grigoriev

et al.

International Conference on Space Optics — ICSO 2018, edited by Zoran Sodnik, Nikos Karafolas, Bruno Cugny, Proc. of SPIE Vol. 11180, 111806O · © 2018 ESA and CNES · CCC code: 0277-786X/18/$18 · doi: 10.1117/12.2536159

Detection Efficiency of Micro Channel Plates and Channel Electron Multiplier Detectors to Penetrating Radiation in Space

N. André[a], A. Fedorov[a], O. Chassela[a], A. Grigoriev[a], E. Le Comte[a], J. Rouzaud[a], M. Bassas[b]
[a]IRAP, CNRS, UPS, CNES, 9 avenue du colonel Roche, 31028 Toulouse, France**;** [b]ISAE, 10 avenue Edouard Belin 31400 Toulouse France

ABSTRACT

Space-based instruments for detection of photons, plasma, and energetic neutral atom imaging include electron multiplier detectors that are subject to increased transient noise, long-term degradation and even potential failure due to the substantial fluxes of high-energy particles that penetrate the instrument in the space environment. The most commonly used electron multiplier detectors are Multi-Channel Plate (MCP) and Channel Electron Multiplier (CEM). These detectors are sensitive not only to the incident energetic charged particles themselves but they are also sensitive to the final end-product energy deposited by energetic electrons, ions, and X-rays. The resulting radiation-induced background noise can potentially swamp the science signal. This issue constitutes undoubtedly the main challenge for particle instruments onboard future missions to Jupiter like the European Space Agency Jupiter ICy moon Explorer (JUICE), and requires dedicated and innovative radiation mitigation techniques (e.g., multiple coincidence, anti-coincidence) far beyond the simple passive shielding techniques commonly used to protect electronics and other subsystems against Total Ionizing Dose (TID). The accurate response (i.e., efficiency) of MCPs and CEMs detectors against high-energy particles is however not well known, with limited estimates available in the literature. This makes it complicated in particular to reliably predict the Signal to Noise ratio of the instrument, and, hence, ensure that the instrument will return useful scientific data when operated in the Jovian magnetosphere. Here, we first use real measurements from the Galileo Plasma spectrometer (PLS) instrument to derive the background noise measured by CEMs in the Jovian environment. These measurements are used in combination with Geant4 simulations in order to estimate the efficiency of CEMs against high-energy electrons. We then present the results of an experiment in which we measured and compared the response of MCP and CEM detectors to keV-MeV electrons and keV X-rays using a Van de Graff electron gun available at ONERA, Toulouse, France. These experimental tests were funded by the french space agency CNES in support of the JUICE mission and in particular for the contribution of the Institut de Recherche en Astrophysique et Planétologie to the Particle Environment Package (PEP).

Keywords: Detectors, Electron multipliers, Space Instrument, Penetrating particles, Radiation

1. INTRODUCTION

Radiation-induced effects on instrument detectors and other key instrument components are significant issues that ultimately impact the quality and quantity of the mission science return and the reliability of engineering sensor data critical to flight operations. A thorough assessment of radiation effects on sensors and detectors of science instruments is therefore needed to ensure data quality for any space mission.

Space particle instruments (e.g., plasma and energetic particle sensors, neutral mass spectrometer, Energetic Neutral Atom imager) and remote-sensing spectrometers (e.g., UltraViolet spectrometer) include electron multiplier detectors that are subject to increased transient noise, long-term degradation, and even potential failure due to the substantial fluxes of high-energy particles that penetrate the instrument. The most commonly used electron multiplier detectors are Multi-Channel Plate (MCP, [1, 2]) and Channel Electron Multiplier (CEM). These detectors are sensitive not only to the incident energetic charged particles themselves but they are also sensitive to the final end-product energy deposited by energetic electrons, ions, and X-rays. The resulting radiation-induced background noise can potentially swamp the science signal [3]).

This issue constitutes undoubtedly the main challenge for particle instruments onboard future missions to Jupiter like the European Space Agency Jupiter ICy moon Explorer (JUICE [4]), and requires dedicated and innovative radiation

mitigation techniques (e.g., multiple coincidence, anti-coincidence) far beyond the simple passive shielding techniques commonly used to protect electronics and other subsystems against Total Ionizing Dose (TID). All plasma–oriented instrument on board the JUICE mission will be exposed to a very hard flow of high energy electrons that fill the Jovian magnetosphere. Since the plasma instruments are located outside the S/C body, it is very difficult to protect the instrument detectors against the penetrating electrons and gamma rays created by the incident electrons in instrument protecting shields. These electrons and gamma rays can create a background noise in the instrument detectors and, if the level of such a noise is rather high, contaminate and corrupt the scientific data. To mitigate such a problem, first of all, we need to know the sensitivity of the instrument detectors to the penetrating electrons and gamma particles. The accurate response (i.e., efficiency) of MCPs and CEMs detectors against high-energy particles is however not well known, with limited estimates available in the literature. This makes it complicated to reliably predict the Signal to Noise ratio of the instrument, and, hence, ensure that the instrument will return useful scientific data when operated in the Jovian magnetosphere.

2. EXPERIMENTAL SETUP

2.1 Experiment general plan and experiment limitation

A strong flow of high-energy electrons in the energy range between 100keV and 100MeV exist in the Jovian environment. Any multilayer protection consisting of layers of Aluminium (Al) and Tantalum (Ta) can reduce the particle flux and modify the incident energy spectrum, but cannot really modify the energy range of the initial and secondary electrons bombarding the MCP or CEM detectors inside the instrument. Moreover we can expect many low-energy (<100 keV) secondary electrons in the vicinity of the MCP or CEM detectors and also photons of about 500 keV of energy. The last particles (gammas) are created in the Ta protection layer.

The MCP efficiency for electrons less then 100 keV of energy is more or less known from the literature [2]. The MCP response to high-energy electrons are less known and can depend on the MCP glass, technology, etc. Thus an “ideal” experiment plan shall be as follows:

- Perform the MCP efficiency measurements for electrons:
  - In the energy range between 50 keV and 100 MeV
  - In the angular range between 0 and 90° to the MCP surface
- Preform the MCP efficiency measurements for the omnidirectional photons of about 500 keV of energy.

2.2 The real experiment setup in ONERA

To perform such measurements we have used the high-energy electron source GEODUR at ONERA, Toulouse, France. There are several limitations in the experiment realization:

- The ONERA source provides the electrons in the energy range between 300 keV and 1500 keV
- Since the original electron beam is rather strong, we have to use the foils to reduce the beam intensity, that can modify the beam energy distribution
- We can create, but we cannot measure the photon flux. We have to use the numerical simulation to estimate the gamma flux striking the MCP surface.

2.3 Detailed Experiment plan/procedure

2.3.1 Experiment outline

To execute the experiment in the ONERA equipment we created a setup shown in the diagram in Figure 1. The original electron beam (on top) passes the attenuation foil and pseudo-uniformly irradiates a PCB with several detectors installed onto the PCB surface (see also Figure 5):

- A MCP sample MCP1 with unprotected entrance surface
- A MCP sample MCP2 of the same type and the same size protected by a special cover (see Figure 3). The cover is made to remove completely the electron flux, but creates the 500 keV photon flow

- A SSD to measure the beam energy distribution
- A Faraday Cap, provided by ONERA, to get the absolute measurements of the incident electron beam

The Detectors PCB is located on the computer controlled turning stage (see also Figure 5).
The preamplifiers of front-end electronics for MCPs and SSD are installed in the vicinity of the PCB inside the vacuum chamber (Figures 2 and 5). The other analog and digital electronics including:

- Amplifiers/discriminators
- computer controlled HV sources
- computer controlled multi-channel analyzer (MCA) to measure the pulse height distribution (PHD) of the MCP output and to measure the SSD spectrum.
- computer controlled counters
- computer controlled voltage sources for discriminator thresholds

are installed outside the vacuum chamber in the special cabinet.

The pictures of the vacuum chamber and the external equipment are shown in Figure 2.

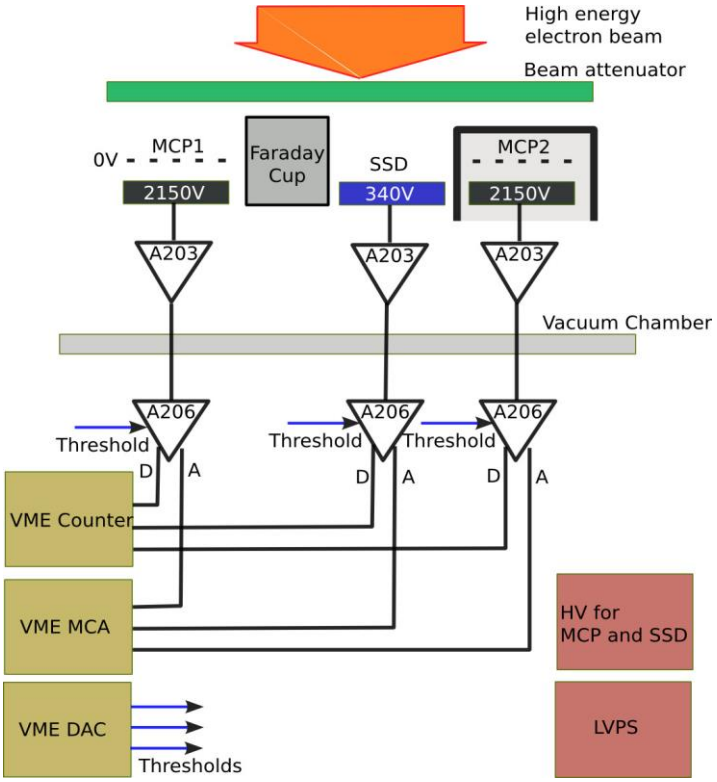

Figure 1. The principal diagram of the experiment

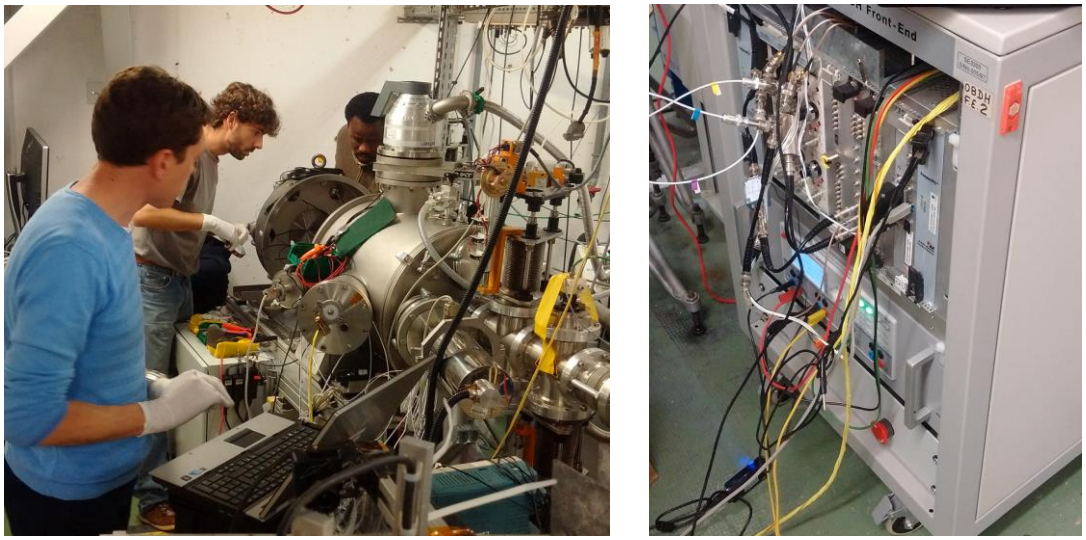

Figure 2. The ONERA vacuum chamber and the experiment support equipment.

The MCP samples information is given in Annex 2.

2.3.2 Experiment procedure (in general)

1. Assessing MCP detection efficiency for high-energy electrons
    a. Set the optimal MCP1 HV and set the optimal discriminator threshold to exclude the noise.
    b. Set the MCP surface normal to the beam axis
    c. For each beam energy from: 400 keV, 700 keV, 1000 keV, 1300 keV, 1500 keV do:
    d. Vary the electron beam intensity from very low to high and register the MCP1 count rate and the incident beam flux. Find the maximal beam flux when the MCP1 count rate is not saturated. Call this point Working Point (WP)
    e. Register the MCP1 PHD at WP
    f. Register the SSD spectrum (as the energy spectrum of the beam) at WP
    g. At WP turn the PCB +/-90° with 15° step and register the MCP1 count
2. Assessing MCP detection efficiency for high-energy photons:
    a. Set the optimal MCP2 HV and set the optimal discriminator threshold to exclude the noise.
    b. Set the MCP surface normal to the beam axis
    c. For two beam energies: 1000 keV and 1500keV do:
    d. Set the maximal beam flux to see the statistically reasonable MCP2 count. Register the beam flux and the MCP2 count rate.

2.3.3 Experiment details

The MCP2 protection shield design is shown in Figure 3. An example of the photon's energy spectrum inside the box is shown in Figure 4. We can see that only 2% of the incident electrons generate the photons. The data are obtained by using the SPENVIS multilayer protection analysis tool.

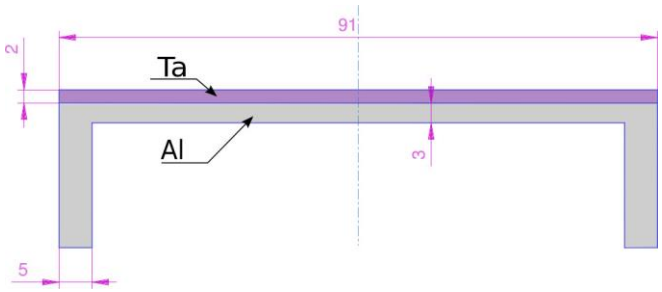

Figure 3 The multilayer MCP2 cover design.

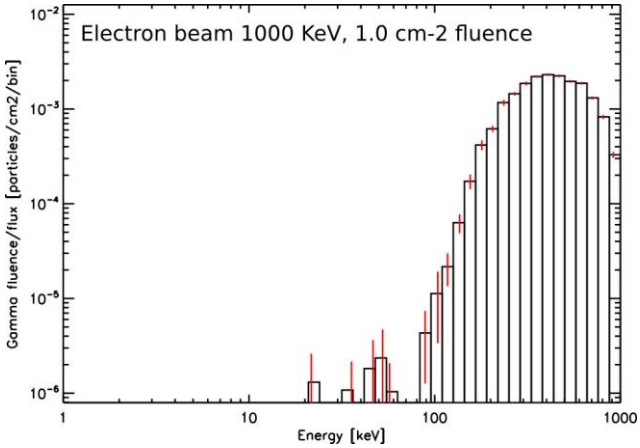

Figure 4 An example of the photon's energy spectra inside the cover.

The real Detector PCB layout and the board installation in the vacuum chamber are shown in Figure 5. The beam intensity and the beam distribution are controlled also by the Al foil installed between the beam source and the detector PCB. The foil modifies the beam slightly. We uses the SSD to check the real incident beam, but it seems that the SSD spectrum sometimes is not absolutely correct due to a SSD saturation. Thus, to get the real incident beam we again rely on SPENVIS simulations.

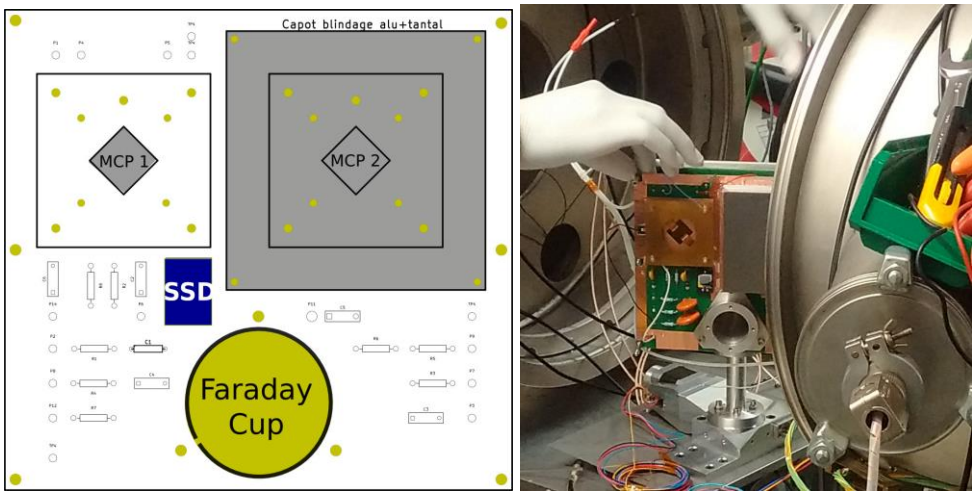

Figure 5 Detector PCB layout (left) and the PCP installed on the turning stage in the vacuum

chamber.

The example of the real beam spectrum is shown in Figure 6. We can see that the real peak intensity becomes smaller but the total beam flux is 12% greater then the original one because of the generation of low-energy secondary ions. We are not going to take into account this feature in the further data analysis.

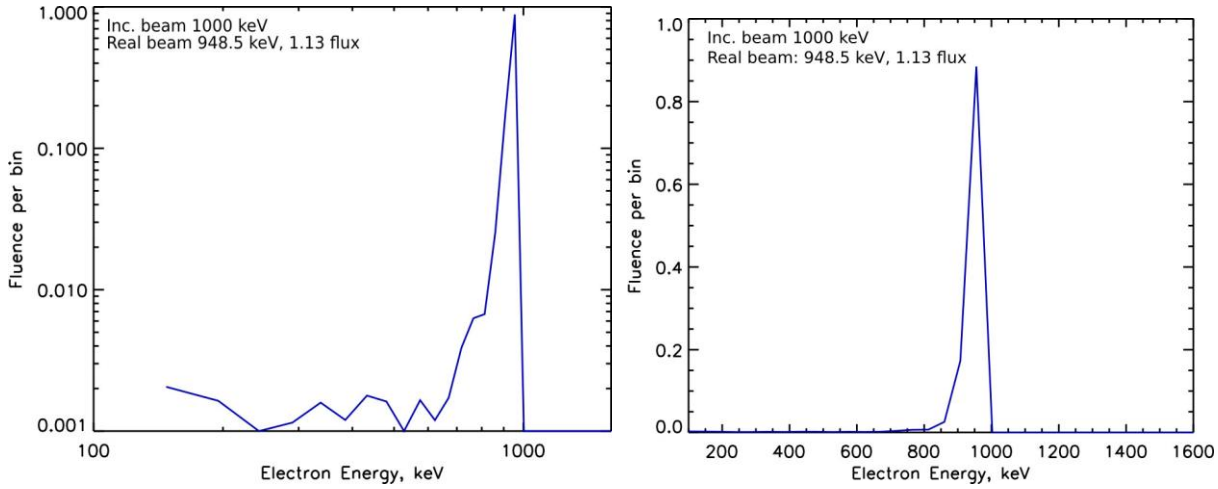

Figure 6 The simulated incident beam spectrum in the log-log scale (left) and in the linear scale (right)

The additional details of the experiment setup are as follows:

1. The Faraday cup surface is 10 cm^2. The minimal ion flux available for the measurements is about 6e3 cm^{-2} s^{-1}. The Working Point beam was usually weaker this limit, and we calculated the real incident beam flux by extrapolation.
2. The MCP 1 and MCP2 area is 2.2 cm2
3. The MCP HV working point is 2150 V for both MCP1 and MCP2
4. The MCP discriminator threshold was set 3.2e6 in terms of the MCP gain for both MCP1 and MCP2. See data analysis section for details.

As it was already mentioned, the MCP samples information is given in Annex 2.

3. EXPERIMENT PROGRESS AND EXPERIMENT DATA

The experiment has been performed on 17 – 21 November 2016 at ONERA.

3.1 MCP Photonis France under the electron beam

Table 1 shows the list of experiments with electrons (the red spectrum is the simulated one):

Orig. beam Energy	Foil	Exp. Label	SSD and simulated beam spectrum
1000 keV	100 µ	A	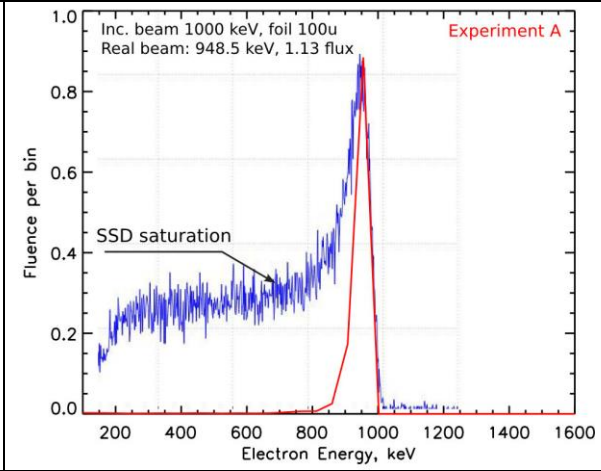
1300 keV	100 µ	B	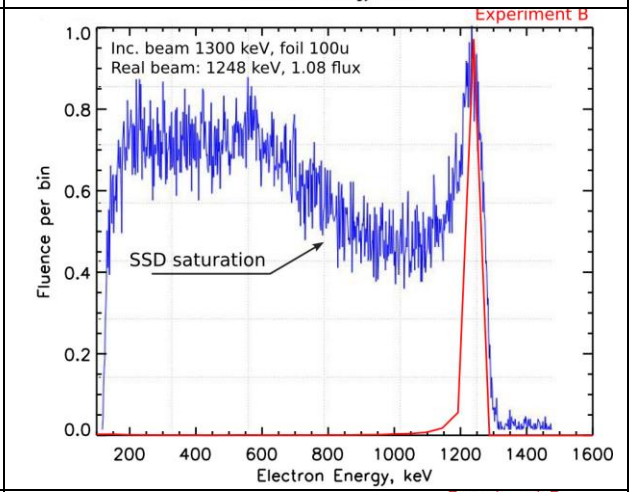
1490 keV	100 µ	C	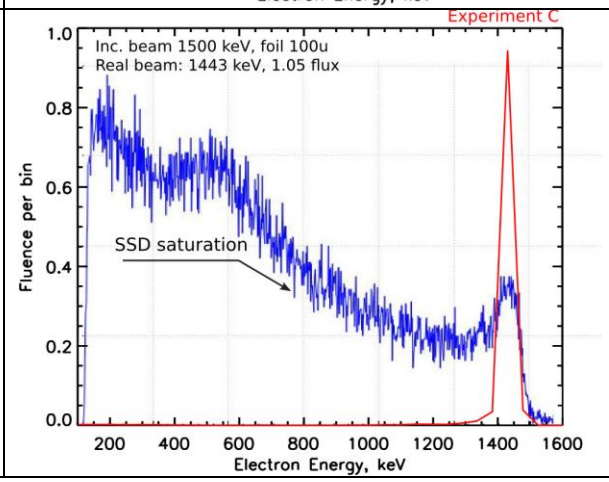

700 keV	100 μ	D	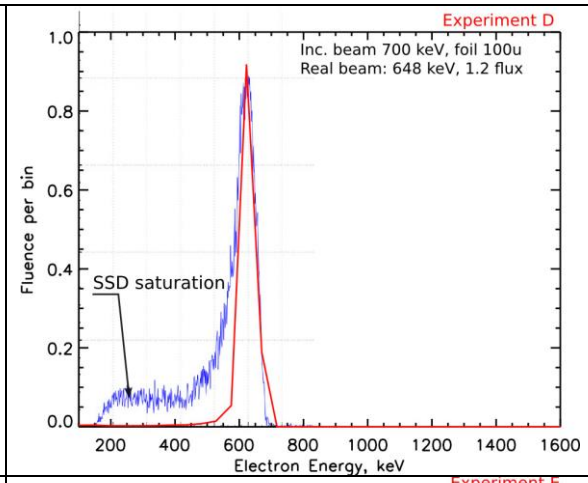
400 keV	30 μ	E	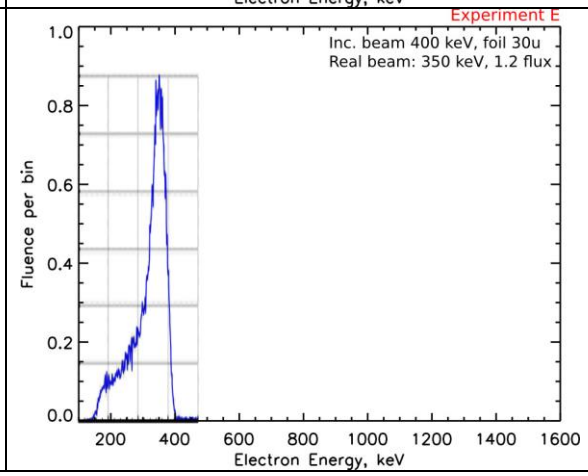

Table 1

The experiment results are shown in Table 2.

Exper.	e- Energ. keV	e- Flux $cm^{-2}\ s^{-1}$	MCP count, s^{-1}	Effic.	MCP PHD
A	948	1.25e4	7.4e3	0.27	NO
B	1248	1.9e4	6.0e3	0.14	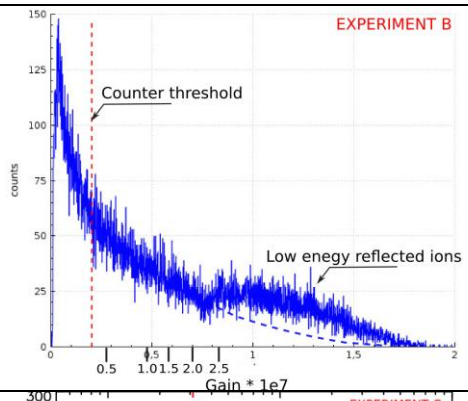
C	1444	2.5e4	6.6e3	0.12	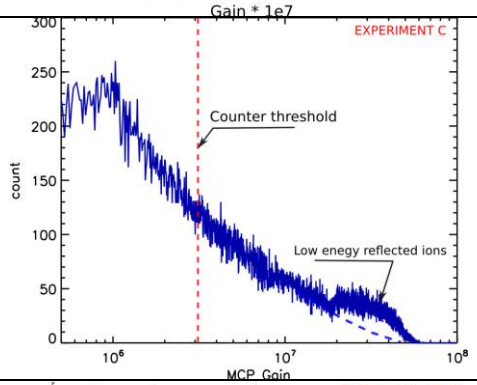
D	649	1.0e4	7.0e3	0.31	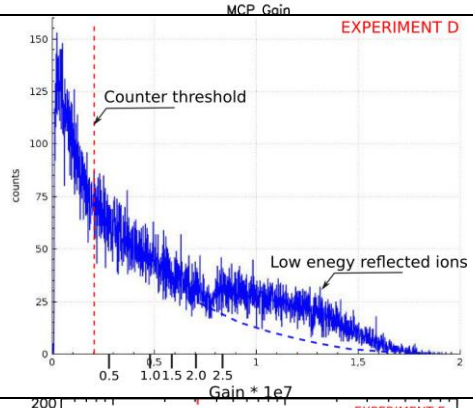
E	350	1.2e4	6.3e3	0.24	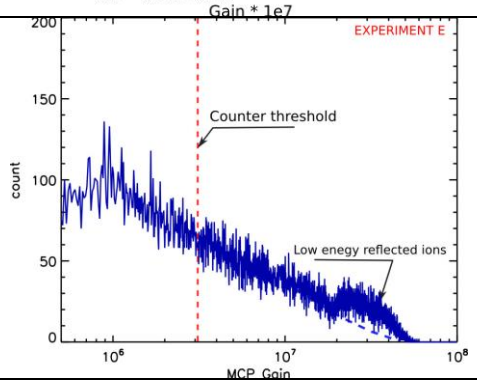

Table 2

We see that the PHD of the events generated by penetrating electron has an exponential shape. A high-energy electron can generate an initial secondary electron at any place inside the micro-channel plate, whereas the low energy particles trigger the secondary electrons at the entrance surface and cause a bell-shape PHD around about 10^7 of gain. We see that some high gain part of the distribution is contaminated by low-energy secondary ions events. We removed this part of the distribution from the efficiency calculations.

3.2 MCP Photonis under the gamma photons beam

The Tables 3 shows the results of the experiment with the gamma particles (protected MCP2).

Exper.	Real γ Energ., keV	γ Flux cm^{-2} s^{-1}	MCP count, s^{-1}	Effic.	MCP PHD
F	443	10.3e4	640	8.8e-4	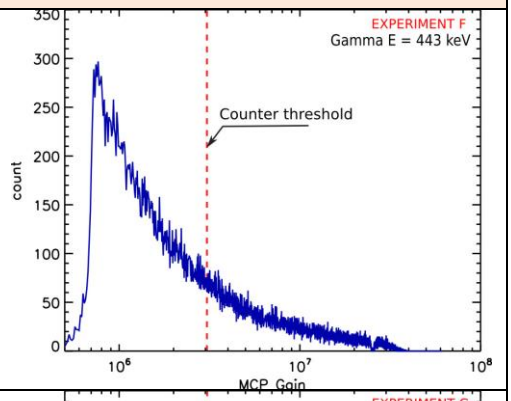
G	547	3.9e4	366	13.1e-4	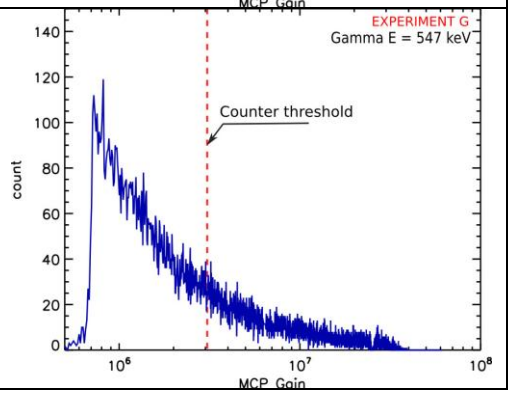

Table 3

4. EXPERIMENT RESULTS AND CONCLUSIONS

Figure 7 shows the test result summary. The red stars show the MCP efficiency to the high-energy electrons, the blue triangles show the same for the gamma radiation. We put here also the results from the publication [3] shown as green circles.

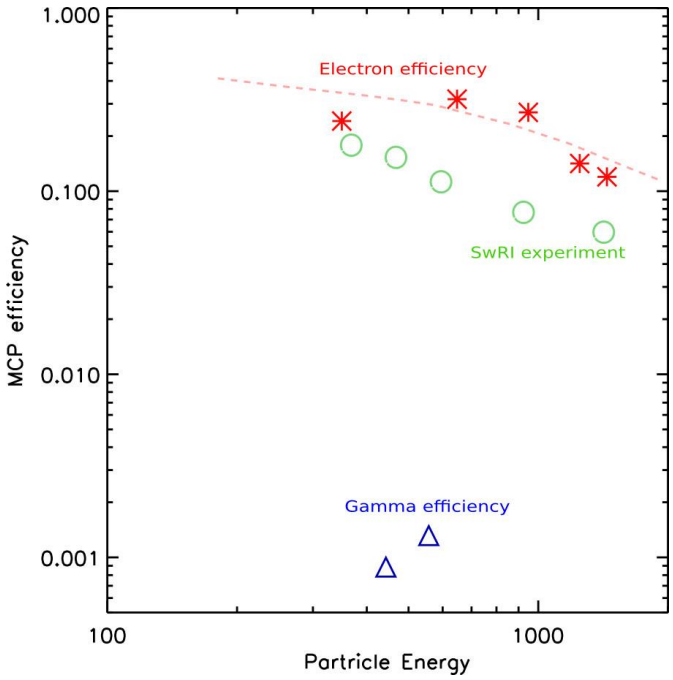

Figure 7. The resulting MCP efficiency plot

Conclusions

1. For the given discriminator threshold the efficiency of the MCP Photonis for the high energy electrons is about 20-30% below 100 keV and going down to 10% for the electron energies greater than 100 keV
2. For the given discriminator threshold the efficiency of the MCP Photonis for the gamma radiation of 500 keV energy is about 0.1%
3. The MCP output PHD is exponential. Thus the MCP efficiency can be varied in the rather wide range by adjusting the threshold.
4. The efficiency variation as a function the incident angle is less then the uncertainty of the presented efficiency at the normal incidence.
5. The efficiency of MCPs against penetrating radiation is significantly higher than the one of ceramic CEM (see Annex 2).

Acknowledgments

These experimental tests were funded by the french space agency CNES in support of the JUICE mission and in particular for the contribution of the Institut de Recherche en Astrophysique et Planétologie to the Particle Environment Package (PEP) through grants Nos 4500046142 and 4500055493.

ANNEX 1: CEM EFFICIENCY TO PENETRATING RADIATION

There are two type of detectors used in space plasma instruments: channeltrons (CEM) and microchannel plates (MCP). Some JUICE plasma sensor teams have chosen the ceramic CEMs since they *a priory* should be less effective to detect penetrating radiation. To obtain ceramic channeltrons (CCEM) efficiency for electrons and X-rays for the energies, specified above, we have tested in 2012 a board with CCEMS from Dr. Sjuts (www.sjuts.com/, Figure 8) in the ONERA GEODUR electron accelerator for energies 0.4 – 1.6 MeV, as well as in the NIST/GSFC (USA) for an energy of 13 MeV.

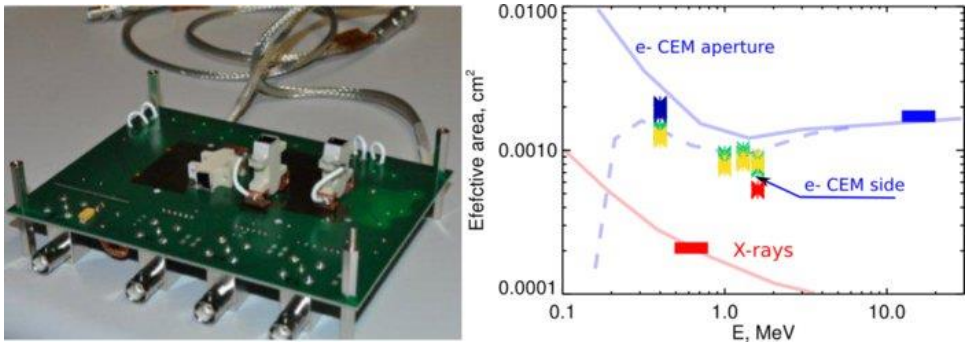

Figure 8. Left: The test board with mounted CEMs. Two CEMs may be covered by an Al-Ta shield. Right: The CEM effective surface (see text for details) as a function of the incident energy. The stars mark ONERA test and the rectangles indicate the GSFC test.

Our test board contained 3 CCEMs. One of them exposed a side to the incident beam and two others pointed their apertures toward the beam. Two CCEMs have been covered by a dedicated shielding of 3 mm Aluminum plus 2 mm Tantalum. During ONERA (low energy) test the side CCEMs was open and during GSFC test the aperture pointed CCEM was open for the incident beam. It each case the absolute value mono-energetic beam flux was known. The "effective aperture" of the CCEM should be a result of the test. The "effective aperture" can be different for the side and the aperture pointed CCEMs.

The aperture is calculated as

$$S_{Eff}\,[cm^2] = \langle \text{Count Rate}[s^{-1}] \rangle / \langle \text{Beam Flux}[cm^{-2}\,s^{-1}] \rangle$$

The results of the experiments are summarized in the right panel of Figure 8. The stars correspond to the direct electron beam striking to a "side" CCEM in the ONERA accelerator. The blue rectangle corresponds to the direct 13 MeV electron beam striking to the CCEM aperture (GSFC). The difference between GSFC and ONERA data are very small. The solid blue curve reproduces a possible profile of the "aperture pointed" CCEM effective area for high-energy electrons. The dashed line reproduces the same for the "side " CCEM. The "side" curve start to deviate from the "aperture" one for low energies and quickly going down for electrons which cannot penetrate into the CCEM. GEANT-4 numerical simulations were used to estimate the electron and X-rays count rate of an idealized virtual omnidirectional detector of 1.5cm^2 averaged surface and 100% efficiency, for an incident electron beam energy of 13 MeV. These simulations show that a CCEM under 3 mm Aluminum plus 2 mm Tantalum shield can detect only bremsstrahlung photons of 500 keV. Thus we can calculate the CCEM photon effective aperture for this important energy. The calculated value has been normalized to the ration between the physical and simulated detector effective area. The final "Photon effective aperture" is shown as a red rectangle in the right panel of Figure 8. One can see that the real CCEM aperture is very small.

ANNEX 2: MCP DATASHEET

For the present test we used four MCP samples of 18x18mm size assembled in two chevron assemblies as shown if Figure 8. These MCP have been cut from the EM JENI MCP batch. The samples data sheet is shown in Figure 9.

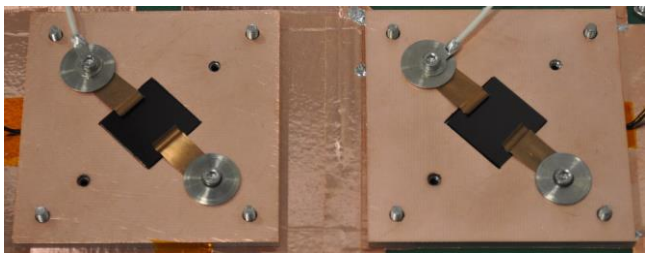

Figure 8. MCP chevron assemblies prepared for the test

PHOTONIS

MICROCHANNEL PLATE

TYPE: G25-18X18MT/12/A/E
NUMBER : YF001-Fb-8 (2)
RESISTANCE: 300 MΩ
METALLISATION: 0.5 / 0.5 ϕ
**** **
VOLTAGE SHOULD BE APPLIED TO THIS
PLATE ONLY UNDER VACUUM CONDITIONS.
****
NOTE: THIS PACKING IS FOR TRANSPORT ONLY
AND SHOULD BE REMOVED IMMEDIATLY.
TO STORE THE PLATE,TRANSFER TO A WATCH-
GLASS SURFACE WITHIN A GLASS PETRI-DISH
AND PLACE IN A DRY NITROGEN CABINET OR
AN OIL-FREE VACUUM CHAMBER.
MATCH WITH : YF001-Fb-8 (1)

PACKED BY: B-C DATE: 14/10/16

PHOTONIS

MICROCHANNEL PLATE

TYPE: G25-18X18MT/12/A/E
NUMBER : YF001-Fb-8 (1)
RESISTANCE: 300 MΩ
METALLISATION: 0.5 / 0.5 ϕ
**** **
VOLTAGE SHOULD BE APPLIED TO THIS
PLATE ONLY UNDER VACUUM CONDITIONS.
****
NOTE: THIS PACKING IS FOR TRANSPORT ONLY
AND SHOULD BE REMOVED IMMEDIATLY.
TO STORE THE PLATE,TRANSFER TO A WATCH-
GLASS SURFACE WITHIN A GLASS PETRI-DISH
AND PLACE IN A DRY NITROGEN CABINET OR
AN OIL-FREE VACUUM CHAMBER.
MATCH WITH : YF001-Fb-8 (2)

PACKED BY: B-C DATE: 14/10/16

PHOTONIS

MICROCHANNEL PLATE

TYPE: G25-18X18MT/12/A/E
NUMBER : YF001-Fb-8 (4)
RESISTANCE: 300 MΩ
METALLISATION: 0.5 / 0.5 ϕ
**** **
VOLTAGE SHOULD BE APPLIED TO THIS
PLATE ONLY UNDER VACUUM CONDITIONS.
****
NOTE: THIS PACKING IS FOR TRANSPORT ONLY
AND SHOULD BE REMOVED IMMEDIATLY.
TO STORE THE PLATE,TRANSFER TO A WATCH-
GLASS SURFACE WITHIN A GLASS PETRI-DISH
AND PLACE IN A DRY NITROGEN CABINET OR
AN OIL-FREE VACUUM CHAMBER.
MATCH WITH : YF001-Fb-8 (3)

PACKED BY: B-C DATE: 14/10/16

PHOTONIS

MICROCHANNEL PLATE

TYPE: G25-18X18MT/12/A/E
NUMBER : YF001-Fb-8 (3)
RESISTANCE: 300 MΩ
METALLISATION: 0.5 / 0.5 ϕ
**** **
VOLTAGE SHOULD BE APPLIED TO THIS
PLATE ONLY UNDER VACUUM CONDITIONS.
****
NOTE: THIS PACKING IS FOR TRANSPORT ONLY
AND SHOULD BE REMOVED IMMEDIATLY.
TO STORE THE PLATE,TRANSFER TO A WATCH-
GLASS SURFACE WITHIN A GLASS PETRI-DISH
AND PLACE IN A DRY NITROGEN CABINET OR
AN OIL-FREE VACUUM CHAMBER.
MATCH WITH : YF001-Fb-8 (4)

PACKED BY: B-C DATE: 14/10/16

Figure 9. MCPs data sheet

REFERENCES

[1] Wiza, J.L., Microchannel Plate Detectors, Nuclear Instruments and Methods, 162, 587-601 (1979)
[2] HAMAMATSU MCP guide
[3] Blase, R.C., Benke, R.R., Cooke, C.M., Pickens, K.S. Microchannel Plate Detector Detection Efficiency to Monoenergetic Electrons Between 0.4 and 2.6 MeV, IEEE Transactions on nuclear science, 62(6) (2015)
[4] Grasset, O., et al., JUpiter ICy moons Explorer (JUICE): An ESA mission to orbit Ganymede and to characterise the Jupiter system, Planetary and Space Science, 78, 1-21 (2013)